Journal of Membrane Science 699 (2024) 122669

Contents lists available at ScienceDirect

Journal of Membrane Science

journal homepage: www.elsevier.com/locate/memsci

Mixed matrix membranes with incorporated glycosaminoglycans have good blood biocompatibility combined to high toxin removal

DooLi Kim [a,d,1], Maria Margalef [b,e,1], Marissa Maciej-Hulme [b,f], Edwin Kellenbach [c], Mark de Graaf [b], Dimitrios Stamatialis [a], Johan van der Vlag [b,*]

[a] Advanced Organ Bioengineering and Therapeutics, Faculty of Science and Technology, TechMed Centre, University of Twente, Enschede, the Netherlands
[b] Department of Nephrology, Radboud Institute for Molecular Life Sciences, Radboud University Medical Centre, Nijmegen, the Netherlands
[c] BioChemOss B.V., FX2123, Kloosterstraat 6, 5349AB, Oss, the Netherlands
[d] Sustainable Process Technology, Faculty of Science and Technology, University of Twente, Enschede, the Netherlands
[e] Amsterdam Institute for Life and Environment (A-LIFE), Vrije Universiteit Amsterdam, Amsterdam, the Netherlands
[f] Department of Life Sciences and Health, Oslo Metropolitan University, Oslo, Norway

ARTICLE INFO

Keywords:
Anti-fouling properties
Biocompatibility
Blending
Coagulation
Hemodialysis
Glycosaminoglycans
Mixed matrix membranes

ABSTRACT

Most patients in need of renal replacement therapy use peritoneal or hemodialysis (HD) therapy. Major drawbacks of HD are the incomplete removal of uremic solutes (especially middle-sized uremic solutes and protein-bound uremic solutes, PBUTs) as well as the non-continuous therapy (3 times per week for 4 h), causing large fluctuations in water balance and uremic waste, potassium, and phosphate. For achieving better patient outcomes, more continuous therapies are required including the application of home HD or portable HD. The latter require membranes with excellent long-term biocompatibility. Heparin-modified dialysis membranes can offer improved biocompatibility, but systemic anticoagulation is still needed, whereas potential heparin-induced thrombocytopenia (HIT) may occur.

Glycosaminoglycans (GAGs) contribute to the kidney glomerular filtration barrier and provide natural anti-fouling properties. Here, we hypothesized that the incorporation of GAGs within polymeric membranes, either via membrane coating, post membrane fabrication, or via blending GAGs into the membrane forming polymer matrix, would provide membranes with improved hemocompatibility. We implemented these strategies to mixed matrix membranes (MMMs) which combine diffusion and adsorption for removing a broad range of uremic solutes. Firstly, we fabricated flat sheet MMMs with various GAG sources, including heparan sulphate from bovine kidney (HSBK), heparinase III-digested HSBK, HS isolated from cultured glomerular endothelial glycocalyx, GAGs from porcine intestinal mucosa (danaparoid, DA), or heparin. The flat sheet MMMs with DA blended within the membrane selective layer have excellent blood compatibility, based on a panel of anti-coagulation and immune activation assays, combined to high water transport and very low albumin leakage. Besides, these MMMs had low clot formation, did not activate immune cells or the complement system and had low platelet adhesion. Based on these findings, we also developed first hollow fiber MMMs with DA blended in the selective layer, which also had high water transport, no leakage of protein, and achieved very good removal of various uremic solutes, comparable to commercial HD membranes.

1. Introduction

Dialysis therapies such as hemodialysis (HD) or peritoneal dialysis are the main renal replacement therapies used to restore the normal blood-filtering function of end stage kidney disease (ESKD) patients. Currently, around 3 million patients receive dialysis treatment worldwide, and the number is expected to reach 5.4 million by 2030 [1]. Despite vast improvements [2], HD is still incomplete and poses great social and psychological burden for the patients due to their recurrent visits to the dialysis center, 3 times per week. Recent advances were

* Corresponding author. Immunology of Kidney Diseases and Transplantation, Radboud university medical center, Department of Nephrology, Geert Grooteplein 10, 6525 GA, Nijmegen, the Netherlands.
E-mail address: Johan.vanderVlag@radboudumc.nl (J. van der Vlag).
[1] These authors contributed equally and therefore share the first authorship.

https://doi.org/10.1016/j.memsci.2024.122669
Received 8 December 2023; Received in revised form 13 February 2024; Accepted 13 March 2024
Available online 14 March 2024

focused on development of miniaturized dialysis machines such as portable or wearable kidney devices [3], aiming to provide more continuous therapy and improve patient daily routine and quality of life. Nevertheless, since the intravascular innate immune system recognizes the synthetic membranes as foreign [4], contact of blood components with the membrane can also trigger blood coagulation in the dialyzer, external and systemic platelet and cell adhesion and activation, complement activation, and thrombosis [5,6]. All these factors can affect the membrane performance [7]. To achieve good biocompatibility of HD membranes various methods have been implemented including coatings, application of suitable polymer blends for membrane fabrication, or membrane surface grafting [8,9]. Besides, efforts have been focused on increasing polymeric surface biocompatibility by application of functionalized materials [10], anti-coagulants [11,12], heparin-mimetic compounds [13–17] or surface amination chemistries [18]. Membrane surface heparinization is quite promising strategy for improving the anticoagulant and antithrombotic properties [13,15,19,20]. However, there is also risk of heparin induced thrombocytopenia (HIT) for these patients [21].

Glycosaminoglycans (GAGs) are a group of linear, sulphated polysaccharides with an uronic acid and amino sugar repeating disaccharide unit, and a variable sulphation pattern. Based on their basic disaccharide structure, GAGs are classified into four groups: heparan sulphate (HS), chondroitin sulphate (CS)/dermatan sulphate (DS), keratan sulphate, and hyaluronic acid [22,23]. Due to its structural diversity, HS is involved in a plethora of different functions, such as the establishment of chemokine gradients [24], reduction of the inflammatory response in anti-glomerular basement membrane nephritis [25] and the localization and regulation of growth factors and cytokines within the sub-endothelial basement membrane [26]. CS/DS are also present in the glomerular basement membrane, but in a much smaller quantity than HS [27]. In addition, interactions have been reported between the HS sulphate groups (negatively charged) with positively charged amino acid residues (such as lysine or arginine) [28]. As heparinase-III is the specific bacterial enzyme that cleaves HS on low sulphated regions, the highly sulphated final fraction might have an increased biological activity.

Due to the well-known contribution of natural occurring GAGs to anti-fouling properties at the kidney glomerulus [29], we hypothesize here that GAG incorporation into the selective layer of a polymeric membrane could improve the anticoagulant and anti-fouling membrane properties [14–16,30–32] and avert the HIT risk [33]. For demonstrating this, we investigated the application of GAGs to mixed matrix membranes (MMMs) which combine filtration and adsorption, have blood compatibility comparable to commercial membranes and have shown higher removal of a broad range of uremic toxins from human plasma *in vitro* [34–37]. In this study for membrane modification, we selected various GAGs, including: HS from bovine kidney (HSBK), heparinase III-digested HSBK (d-HSBK), HS isolated from cultured glomerular endothelial glycocalyx (HS-Glx) as renal sources of HS, danaparoid (DA), a mixture of GAGs from porcine intestine containing mainly low molecular weight HS [38], which is a heparin substitute when patients suffer from HIT [33,39].

Firstly, we developed flat sheet MMMs for selecting the optimal GAG and for assessing the optimal method of GAG incorporation to the membrane. For the latter, two different approaches were employed. The first involved coating the GAGs onto the sorbent-free layer of pre-existing MMMs. The second entailed blending the GAGs into the sorbent-free polymer solution, followed by MMMs fabrication. The new MMMs were characterized concerning membrane morphology, transport properties (pure water permeance, albumin sieving coefficient) and blood compatibility (panel of anti-coagulant assays, and activation and adhesion of blood components) and were compared to membranes without GAGs, to control membranes currently used in the clinic, or positive controls spiked with common blood activators. Finally, based on the best results of the flat sheet MMMs, we developed first MMM hollow fibers with GAGs which were also characterized extensively concerning morphology and transport properties, including removal of uremic solutes (creatinine and two protein bound uremic toxins (PBUTs): indoxyl sulphate and hippuric acid) from human plasma. These results were compared with membranes currently used in the clinic (FX1000, Fresenius).

2. Materials and methods

2.1. Isolation of HS from mouse glomerular endothelial glycocalyx

2.1.1. Cell culture

Conditionally immortalized mouse glomerular endothelial cells (mGEnCs) were cultured, as previously described [40]. Briefly, proliferative mGEnCs were grown in 1 % Gelatin (Merck) pre-coated culture flasks (Corning Life Sciences) at 33 °C and 5% CO_2 with DEMEM/Ham's F12 medium (3:1, Life Technologies) supplemented with 10 % foetal bovine serum (FBS, Bodinco), 1% penicillin/streptomycin (P/S, Life Technologies) and 20 units (U)/mL recombinant mouse interferon-γ (IFN-γ, PeproTech). Subsequently, mGEnCs were seeded for differentiation at 25% density and grown at 37 °C for 7 days in DEMEM/Ham's F12 medium supplemented with 5 % FBS, 1% P/S in uncoated cell culture flasks. In all conditions, media were refreshed every two days.

2.1.2. Isolation of GAGs from cells

Confluent cell monolayers were washed with phosphate-buffered saline (PBS) and digested overnight at 37 °C with proteinase K (8.9 $\mu g/cm^2$, Merck) in extraction buffer (50 mM Tris-HCl, 10 mM NaCl, 3 mM $MgCl_2$, and 1% Triton X-100, pH 7.9). Lysate was recovered from the culture flask and heated to 95 °C for 10 min to stop the proteolysis before adding DNase-I (7.5 U/mL; Qiagen) and RNase (10 U/mL; ThermoFisher Scientific) overnight at 37 °C. The digested lysate was mixed 1:1 (v/v) with 4 M NaCl to dissociate GAG-bound peptides, and subsequently 1:1 (v/v) with chloroform following a centrifugation at 4500×*g* for 30 min to phase/separate the lipidic fraction. The aqueous GAG-containing fraction was collected, dialyzed against 18.3 MΩ cm deionized water (MQ), and dried completely using a SC200 SpeedVac centrifugal evaporator (Savant Instruments).

2.1.3. Anion exchange chromatography for HS purification

The dried GAG-containing fraction was dissolved in digestion buffer containing 50 mM Tris-HCl, 4 mM Mg $(Ac)_2$, pH 8.0 (0.1 m^2/mL). Chondroitin sulphate was digested for 24 h at 37 °C using a double spiking of CABCase (250 mU/m^2; Merck). The enzymatic digestion was deactivated by heating the sample to 95 °C for 10 min. Digested sample was dialyzed and dried completely as described above. Dried digested sample from 1 m^2 of cultured cells was dissolved in 150 mL PBS. Solution was applied to a 100 mL Di-Ethylaminoethanol (DEAE)-Sepharose CL-6B (Merck) column pre-equilibrated with PBS. Non-specific interactions with the DEAE beads were removed with 0.25 M NaCl in PBS. The HS-Glx fraction was eluted with 2 M NaCl in PBS, collected, dialyzed, and dried completely as described above.

2.2. Membrane preparation

2.2.1. Materials

Polyethersulfone (PES, Mw = 60 kg/mol, Ultrason E6020P, BASF), polyvinylpyrrolidone (PVP, Mw = 360 kg/mol, Merck), 1-methyl-2-pyrrolidone (NMP, Merck) were used for both the sorbent free polymer solution and for the sorbent-based polymer solution together with activated carbon (AC, Norit Netherlands B.V.). For protein transport studies, α-lactalbumin (Mw = 14.2 kg/mol, Merck), β-lactalbumin (Mw = 36.8 kg/mol, Merck), and bovine serum albumin (BSA, Mw = 66.5 kg/mol, Merck) were employed. For the toxin removal studies, creatinine (Cr, Mw = 113 g/mol, Merck), indoxyl sulphate (IS, Mw = 251 g/mol, Merck), hippuric acid (HA, Mw = 179 g/mol, Merck) and human plasma

(Sanquin, Deventer, The Netherlands) were applied. For the transport studies, a lab made dialysate solution (all salts, Merck) was used and all chemicals (KCl, NaCl, $CaCl_2$, $MgCl_2$, $NaHCO_3$, and glucose) were purchased from Merck. A commercial membrane, Fresenius, FX1000 dialyzer, was employed as a reference to compare the performance and toxin removal of the developed MMMs.

2.2.2. Preparation of polymer solutions

PES and PVP were dissolved in 1-methyl-2-pyrrolidone (NMP) at room temperature (RT) for 24 h to obtain a sorbent free polymer solution. Two types of the sorbent free polymer solutions were prepared, without GAGs and with blending of DA or HS, see Table 1. For the GAG blending, DA (30 and 60 mg/ml in water) or HS (60 mg/ml in water) solutions were prepared and were added as additives in the polymer dope (5 wt% of the GAG-water solutions over the total polymer solution was added in the preprepared polymer solution of 20 wt% PES/2 wt% PVP/73 wt% NMP). The sorbent-base polymer solution was prepared by adding activated carbon (Norit Netherlands B.V.) to an already made homogeneous PES/PVP/NMP polymer solution. This sorbent-based polymer solution was mixed in a roller bank for 48 h at RT to obtain a homogeneous solution. All polymer solutions were degassed for 24 h prior to the MMM fabrication. Table 1 shows the polymer compositions of all polymer solutions used for the MMM fabrication.

2.2.3. Flat sheet MMMs

The polymer solutions, without and with sorbent, were cast on a glass plate at the same time with two casting knifes, having gaps of 0.15 and 0.3 mm, as described previously [34]. Subsequently, the cast MMM was immediately immersed in non-solvent, water, to form the MMM. The membranes were then rinsed with MiliQ water to remove residual solvent traces and stored in MiliQ water upon further use.

For GAGs coating, the MMM was cut to size (0.96 cm^2 and 9.5 cm^2) with circular punchers and placed into Costar® sterile 48-well and 6-well culture plates (Corning Incorporated) for the biocompatibility assays. All MMMs were fixed on the bottom of the culture plates with fluoro-elastomer O-rings (Eriks). This allowed an optimal flatness of the surface for a homogeneous coating and biocompatibility assay procedures. These MMMs were rinsed 5 times in 70% ethanol solution and kept in sterile MiliQ water until needed. Before coating, they were washed 3 times with sterile phosphate buffer saline (PBS). Prior all the biocompatibility assays, the MMMs were washed 5 times with sterile distilled ultra-pure water.

Various GAGs were used for membrane coating: (a) HSBK (30 μg/mL, Merck), (b) HSBK partially digested after incubation with Heparinase-III (0.2U/μg, IDURON) for 30 min at 37 °C (d-HSBK, 60 μg/mL), (c) HS-Glx (200 cm^2 extracted cells/mL) and (d) DA (400 μg/mL, Aspen Oss). Note, different GAG concentrations were chosen depending on the highest coating efficiency of each GAG. The MMMs were incubated overnight at RT with the different GAG solutions. Afterwards MMMs were rinsed 3 times with fresh sterile HS coating buffer.

For the GAG blended MMMs, the sorbent free polymer solution mixed with HS and DA (see Table 1) was selected and the fabrication procedure was the same as the standard flat MMM. A homogeneous PES/PVP/NMP polymer solution (20/2/73 wt%), an aqueous solution of DA (60 mg/mL) or HS (60 mg/mL for comparison, Merck) were prepared separately. The sorbent free polymer solution was prepared by adding 5 wt% of DA or HS- aqueous solutions into the PES/PVP/NMP polymer solution and mixed for 48 h at RT using a roller bank. The sorbent-based polymer solution and the final GAG-blended MMMs were prepared with the same method of the standard MMM.

The GAG release from the MMMs (coated and blended) was also studied over time. These MMMs were incubated in MQ water at 37 °C under shaking conditions (100 rpm) for 4, 8 and 24 h. The supernatants were collected, and their GAG concentrations were analyzed via ELISA. Briefly, supernatants were subjected to an ELISA assay using the VSV-tagged single chain anti-HS antibody EW4G2 (REF), and absorbance at 450 nm was measured using a Benchmark plus micro plate spectrophotometer (BioRad). The GAG release was studied using specific standard curves of each GAG source and extrapolating the absorbance from the solution before and after coating.

DA-modified MMMs were also specifically stained using the VSV-tagged single chain anti-HS antibody HS4C3 [41], and cryo-sectioned with a HM560 CryoStar Cryostat (Thermo Scientific). The presence of GAGs on the different MMMs was accessed on a Zeiss Axio imager M1 (Zeiss) immunofluorescence microscope using standard filter sets.

2.2.4. Hollow fiber (HF) MMM

Two dope solutions were spun simultaneously to fabricate dual layered HF MMMs. The employed spinning conditions (see Table 2) were based to those reported earlier [36]. After spinning, the HFs were immersed in Milli-Q water. To ensure the removal of residual solvent traces, the water was replaced with fresh water on an hourly basis during the first 2 h. Subsequently, the HF MMMs were stored in Milli-Q water for further use.

For the membrane transport studies, we prepared modules with 10 HF membranes each. The total length of the module ranged between 8.5 and 12 cm. Epoxy adhesive (Griffon Combi) consisting of epoxy resin and hardener was used to pot the two ends of the modules. The effective surface area of the HF membranes was determined by subtracting the combined length of the two glued ends, approximately 2 cm per glued end, from the initial module length. To make a lab scale commercial membrane module for a fair comparison, we autopsied a commercial dialyzer (FX1000, total effective membrane area of 2.2 m^2) and made lab scale modules with 10 HFs too.

2.3. Membrane characterization

2.3.1. Membrane morphology

Scanning electron microscopy (SEM) was used to investigate the MMM morphology. For this, the developed flat and HF MMMs were fractured using liquid nitrogen and subsequently coated with gold using a sputter coater (Cressington 108 auto sputter coater) to obtain cross-sectional images using a JEOL JSM-IT100 scanning electron

Table 1
The composition of polymer dope for the MMM preparation.

MMM composition	PES (%)	PVP (%)	NMP (%)	AC (%)	Danaparoid or heparin in water (%)
Sorbent free layer-no GAGs	20	2	78	N/A	N/A
Sorbent free layer + GAGs	20	2	73	N/A	5 (30 or 60 mg/ml)
Sorbent based layer	14	1.4	84.6	60[a]	N/A

[a] The concentration of AC is 60 % of the total polymer amount (PES and PVP).

Table 2
HF MMMs spinning conditions.

Spinning condition		HF-DA60W	HF-DA30W
Composition	Inner	15% PES/7% PVP/5 % DA-water (60 mg/ml)/73% NMP	15% PES/7% PVP/5 % DA-water (30 mg/ml)/73% NMP
	Outer	14% PES/1.4% PVP/NMP/60% AC	
	Bore	Water	
Flow rate	Inner (ml/min)	0.1	
	Outer (ml/min)	0.2	
	Bore (ml/min)	0.2	
Air gap (cm)		34	
Take up (m/min)		Free falling, 0.35 (1.5–1.8 V)	

microscope (JEOL).

2.3.2. Water transport

The water transport across the MMMs was measured at 2 bars for 1 h using a dead-end filtration set-up. The membrane water permeance (L m^{-2} h^{-1} bar^{-1}) was estimated by the following equation:

$$\text{Water permeance } (L/m^2 \text{ h bar}) = Q \times A^{-1} \times \Delta P^{-1} \tag{1}$$

where Q is the water flux through the membrane (L/h), A is the effective membrane area (m^2), and ΔP is the applied transmembrane pressure (TMP in bar). From these results, we also estimated the membrane ultrafiltration coefficient (K_{UF}, ml/(m^2 h mmHg)).

2.3.3. Protein sieving coefficient

The transport of α-lactalbumin (Mw = 14.2 kg/mol), β-lactalbumin (Mw = 36.8 kg/mol) and bovine serum albumin (BSA, Mw = 66.5 kg/mol) across the MMM was measured at 2 bars for 1 h using a dead-end filtration set-up. The concentration of all protein feed (C_{feed}) solutions was 1 g/l. The protein sieving coefficient (SC) of the membranes was estimated using the following equation:

$$SC = \frac{C_{perm}}{C_{feed}} \tag{2}$$

where C_{perm} and C_{feed} are the concentrations of the permeate and feed protein solutions, respectively, which were analyzed by UV Spectroscopy (Nanodrop).

2.3.4. Toxin removal from human plasma

The removal of the uremic toxins from human plasma by the HF membranes was studied. Plasma of 3 healthy donors (Sanquin-Deventer, The Netherlands) was spiked with creatinine (Cr, 136 mg/L), indoxyl sulphate (IS, 40 mg/L), and hippuric acid (HA, 110 mg/L) and was incubated for 4 h at 37 °C under gentle shaking. The concentrations of toxins were selected based on the data from the European Uremic Toxin Work Group (EUTox) of the European Society for Artificial Organs (ESAO) [42].

A standardized protocol with 3 steps was employed for the toxin removal test. Initially, a pure water flux was measured to maximize the pore opening and the membrane wettability. Subsequently, an *in vitro* HD session was performed over a duration of 24 h in a lab scale HD system (Convergence inspector) to assess the removal of toxins through MMMs. For this, a lab-made dialysate: KCl (2 mM), NaCl (140 mM), $CaCl_2$ (1.5 mM), $MgCl_2$ (0.25 mM), $NaHCO_3$ (35 mM), and Glucose (5.5 mM) was employed. During the hemodialysis session, the flow rates of both the human plasma and dialysate were strictly controlled at 1 and 2 ml/min, respectively, while the TMP was maintained at 0 bar. Finally, after the HD session, the pure water flux was again measured to assess membrane fouling or other related phenomena.

To quantify the toxin removal, 1 ml samples were collected from both the human plasma and dialysate every hour for the initial 4 h, as well as at 24 h. To prepare the collected samples for analysis, a four-fold dilution was performed using deionized water, followed by deproteinization through heat denaturation at 95 °C for 30 min. Subsequently, the samples were rapidly cooled in an ice bath for 15 min and transferred to centrifugal filters (Millipore, MWCO 10 kg/mol) to separate the denatured protein from the liquid containing the toxins. Centrifugation was conducted at 14,000 RCF for 15 min. The concentrations of Cr, IS and HA were determined using high performance liquid chromatography (HPLC, Jasco) equipped with UV and fluorescence detectors along with a XBridge BEH C8 column (2.5 μm particle size, 4.6 × 150 mm dimensions). Additionally, to evaluate any potential protein leakage, the protein concentration of samples collected from the dialysate during the 24-h HD session was assessed using UV-spectroscopy (NanoDrop).

2.4. Biocompatibility assays

2.4.1. Blood coagulation time

20 mL of whole blood from 3 healthy volunteers was collected in citrated BD Vacutainer tubes (Beckton Dickinson) and centrifuged at 400×*g* for 10 min at RT to separate the blood corpuscles. Then the platelet rich plasma (PRP) was centrifuged at 3000×*g* for 10 min at RT to pellet down the platelets and obtain platelet poor plasma (PPP). Coated and blended MMMs were incubated with 0.5 mL of PPP for 1 h at 37 °C and the prothrombin time (PT) and activated partial prothoplasmin time (aPTT) of the PPP were then determined using a CA-50 automated blood coagulation analyzer (Sysmex Corp.).

2.4.2. Anti-factor Xa activity

The anti-factor Xa activity associated with the membranes was performed using a Stachrom© Heparin kit (Diagnostica Stago) and following previously reported adaptations [32]. Briefly, duplicate MMMs were incubated with antithrombin (AT) solution at 37 °C for 10 min, to allow the AT-GAG complex formation. A known excess of factor Xa was added for 5 min. Subsequently, 60 μL of the solution, and 60 μL of the known excess of factor Xa (negative control) were transferred to the wells of a 96-well plate containing 60 μL of the factor Xa chromogenic substrate CBS 31.39. When the residual factor Xa reacts with the chromogenic substrate the released amount of paranitroanaline (pNA) can be directly related to the anti-factor Xa activity of the surface. Absorbance of the solutions was measured at 405 nm to obtain a representative value of the residual factor Xa and results were normalized against the signal of the initial factor Xa (negative control). The experiment was performed in triplicate.

2.4.3. Thrombin binding and fibrinogen deposition

Two different sets of MMM were used for thrombin binding experiments, and fibrinogen deposition experiments. An indirect ELISA using anti-human thrombin antibody (Abcam) was used to determine the thrombin binding to the modified MMM. To determine the deposition of fibrinogen on the MMM, a direct ELISA was performed using FITC-conjugated anti-human fibrinogen antibody (Abcam). For both studies, PPP from 3 different healthy volunteers was obtained MMMs were incubated with 250 μL of PPP for 1 h at 37 °C. After incubation MMMs were washed to discard any non-adherent components and incubated with the respective antibodies (anti-human thrombin antibody + anti-IgG-Alexa Fluor 488, or FITC-conjugated anti-human fibrinogen antibody). Fluorescence was measured on the MMM containing 200 μL of PBS using an Infinite 200 PRO plate reader (Tecan Trading AG). Excitation and emission wavelengths used in for thrombin binding were 495 nm and 519 nm respectively. Excitation and emission wavelengths used in for fibrinogen deposition were 493 nm and 528 nm respectively.

2.4.4. Complement activation

As artificial surfaces are known to activate the complement system, complement activation were measured by the quantification of C5a in serum samples using a human Complement C5a ELISA kit (Abcam). Briefly, blood from 3 different healthy volunteers was collected in Vacutainer tubes with no anticoagulant and left to clot for 30 min at RT. Serum samples were obtained by centrifugation of the whole blood at 1500×*g* for 10 min. MMMs were incubated with 250 μL of serum at 37 °C for 1 h. Furthermore, regenerated cellulose (RC) membranes (Whatman), previously used for HD and reported to significantly activate the complement system [43], were also incubated with serum as a positive control. After incubation, C5a serum content was analyzed according to the instructions of the manufacturer.

2.4.5. Blood cell activation and adhesion

The blood cell activation and adhesion were measured by two different approaches after the incubating modified MMMs with 200 μL of whole blood at 37 °C for 1 h, under shaking conditions: (i) measuring the formation of reactive oxygen species (ROS) in whole blood by a luminol based ROS assay, and (ii) studying cell count and different markers in whole blood by flow Cytometry. Fresh whole blood was collected from three different healthy volunteers In addition, whole blood samples containing 8 μM of phorbol 12-myristate 13-acetate (PMA, Merck), or 10 ng/mL of lipopolysaccharide (LPS, Merck) were also incubated at 37 °C for 1 h as a positive control.

For the luminol based ROS assay, 200 μL of 1:100 diluted blood with Hank's balanced salt solution (HBSS, Gibco, Thermo Fisher Scientific) were added to the wells of a 96 well plate containing 20 μL of luminol (Merck). Luminescence was immediately measured at 425 nm in a 37 °C pre-warmed Synergy HT micro plate reader (Biotek) for 1 h.

For the flow Cytometry assay, 50 μL of blood were added to polypropylene tubes and incubated at RT for 20 min with directly labelled monoclonal antibodies CD64-FITC, CD56-PE, CD3-PacificBlue, CD66b-PerCP/Cy5.5, and CD54-APC (Biolegend), and CD20-Pe/Cy7 and CD69-APC/Cy7 (BD Pharmigen), or with isotype matched. CD64, CD56, CD3, CD20, and CD66b were used as cell differentiation markers of monocytes, natural killers (NK), T and B-cells, and neutrophils respectively. CD54 was used as a cell activation marker for monocytes and neutrophils, and CD69 was used as a cell activation marker for NK, T and B-cells. After incubation, 1 mL of FACSlyse solution (BD Biosciences) was added, samples were incubated at RT for 10 min in the dark. Then samples were centrifuged at 400×*g* for 5 min. After two washing steps with 1% Bovine Serum Albumin in PBS (PBA), cells were resuspended in PBA and the expression of different receptors was read by flow Cytometry. The total living cell population was gated according to the forward and side-scatter light profiles. The different cell populations were gated according to their specific cell differentiation marker and the side-scatter light profile. Cell activation was assessed by double gating of cell differentiation/activation markers. Fluorescence was measured on the green, yellow, and blue channels, and all gates were adjusted to a single quadrant (MMM with no GAGs – differentiation$^+$/activation$^-$). Population shifts in activation were evaluated in the different MMM configurations (an example of the gating strategy is presented in Fig. S1). Compensation was performed using a VersaComp Antibody capture bead kit (Beckman Coulter Life Sciences) following the instructions of the manufacturer. Cell adhesion was evaluated by gating of the forward and side-scatter light profile and comparing the results and analyzing the total cell count. Each sample was analyzed for 150 s. A minimum of 10000 events were collected, and data were recorded as mean fluorescence channel number. Median Fluorescence Intensity (MFI) values were multiplied by the percentage of gated cells in the population for each individual donor. Results were normalized against the unmodified MMM to obtain the cell activation fold-change.

White blood cells adhesion was studied by flow cytometry using the events (gated living cell population) count before and after incubation. Results from the samples incubated on the different MMM configurations were subtracted from the results of fresh non-incubated samples. The obtained difference was directly related to the number of cells adhered on the membrane surface. Results were compared against unmodified MMM. All flow cytometry analysis was performed using a CytoFLEX benchtop flow cytometer (Beckman Coulter Life Sciences), and data analysis was performed by Kaluza 2.1 software.

Platelet adhesion was quantified using the pierce lactate dehydrogenase (LDH) cytotoxicity assay kit (Thermo Fisher Scientific). PRP was obtained from 3 different healthy volunteers. MMMs were incubated with 150 μL of PRP (35-45 x 10^6 platelets/mL) at 37 °C for 1 h. Afterwards, PRP was aspirated and MMMs were washed 3 times with sterile PBS to remove non-adherent platelets. Then 150 μL of lysis buffer were added to the MMM for 1 h, at RT. Subsequently 50 μL of supernatant were transferred to a 96 well plate and 50 μL of substrate mix were added for 30 min. Finally, 50 μL of stop solution were added and absorbance was measured at 490 nm and 680 nm. To determine LDH activity, the background signal from the instrument (absorbance at 680 nm) was subtracted from the sample signal (absorbance at 490 nm). The number of adherent platelets was quantified by a plotted standard curve from serial diluted samples containing known amounts of platelets determined with a CASY TTC cell analyzer (OLS OMNI Life Science).

2.5. *Statistical analysis*

Statistical significance was set at 3 different levels (*$p < 0.05$, **$p < 0.01$, and ***$p < 0.001$), and assessed by one-way ANOVA using Dunnett as a *post-hoc* or *t*-Student tests using GraphPad PRISM (version 5.03). All data are expressed as mean ± standard deviation (SD) from at least 2 technical replicates or mean ± standard error of the mean (SEM) from 3 biological replicates.

3. Results and discussion

3.1. *Flat sheet MMM*

Fig. 1 presents typical SEM images of the unmodified (without GAGs) flat sheet MMM that consists of two layers: the sorbent-free layer (top layer), and the layer with activated carbon (AC) sorbent particles (bottom layer). The adhesion between the two layer is very good (no delamination occurred). The sorbent free layer had an asymmetric porous structure, with a dense top selective layer followed by an area with finger like pores. The AC is well distributed within the bottom layer, which presented a rather spongy structure.

3.2. *Flat sheet MMM with GAGs*

For the GAG coated MMMs, the sorbent free layer of the MMMs was coated with different GAG preparations. The efficiency before and after coating were compared in Table S1. DA, d-HSBK and HSBK showed higher coating percentages on the MMMs (92, 95, and 93% respectively). The coating of HS-Glx was low (26 %).

The concentration of the GAG aqueous solution, which was mixed to the sorbent free polymer solutions, was decided by cloud point tests. Briefly, water as a strong non-solvent was gradually added in the sorbent free polymer solution. When the addition of water reached to 6.3 %, the polymer solution became turbid (cloud point) and phase separation occurred. Based on this, to avoid de-mixing, during membrane solution preparation, we selected 5 wt% GAG aqueous solution for the blending. The MMMs with DA and HS had efficiency of 96%, and 99% respectively (Table S1), besides over a 24-h period there was hardly any release of DA from the coated or DA-blended MMMs (Table S1).

The top selective layer of the MMM blended with DA is thicker (approximately 5.5 μm) than the unmodified MMM, see Fig. 2A, which is probably caused by the addition of water (a strong non-solvent). The adhesion between the two layers was again very good without defects or delamination and AC was dispersed homogenously within the polymer matrix. The presence and localization of DA to the membranes was confirmed using immunofluorescence microscopy (Fig. 2B). The results showed that DA for the MMMs was mainly located on the surface of the membrane (red line: Fig. 2B left panel), but also diffused into the polymeric layer (Fig. 2B right panel).

3.3. *Characterization of flat MMMs*

The unmodified MMMs had high water permeance (184 ± 68 L/h m^2 bar) with low albumin leakage ($SC_A = 0.03 \pm 0.03$). After coating with HSBK, differences were observed on the water transport capacity, but not for the albumin selectivity (Table 4). All the other MMMs have high water transport and low albumin leakage, similarly to the unmodified MMM. The charge difference between the different GAG sources may increase the wettability and hydrophilicity of MMMs, explaining the differences observed in the HSBK-coated membranes. (Table 3). GAGs are linear polysaccharides that consist of repeating disaccharide units. Their primary chemical functional groups include polar functional

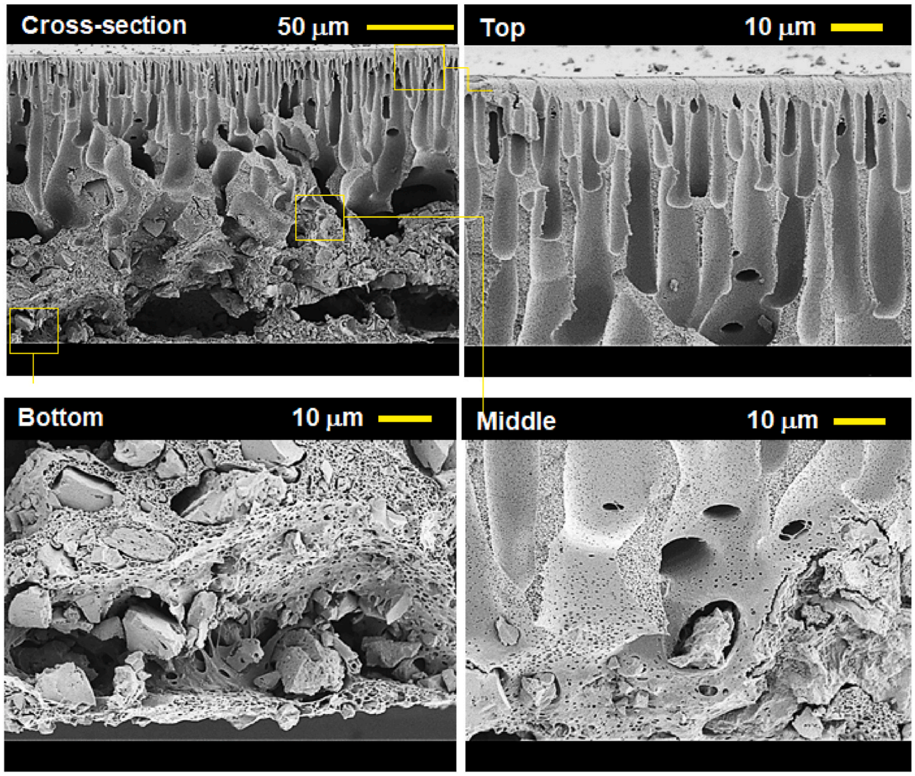

Fig. 1. SEM images of the standard MMM: the top (x 500), middle (x 1500), and bottom (x 1500) part. No defects between the two layers and well distributed solvents can be seen.

groups such as carboxylic acid, hydroxyl, amino, and sulphate groups, hence it is expected to improve membrane hydrophilicity. There is significant amount of literature supporting this. For example, Ren et al., studied heparin immobilized polysulfone membranes and reported that the contact angle was significantly reduced from 87° to 30° after heparin immobilization, but due to the swelling of membranes, the improvement of the water permeability was not significant [44]. Huang et al., also showed that immobilized heparin on polysulfone membranes decreases their contact angle (from 95° to 49°) and increases their wettability [45]. H. Baumann et al., developed heparin modified polysulfone membranes and reported that introduction of heparin increased the wettability and improved the flux properties of these membranes [46]. The water transport of membranes coated with d-HSBK is much lower than those of membranes coated with HSBK. We think that the membrane coating using larger amounts of d-HSBK (based on the coating efficiencies, see Tables S1 and 57 μg/mL of d-HSBK compared to 28 μg/mL of HSBK) combined with its shorter disaccharide repeating units, compared to HSBK, results to a denser coating layer which limits the water transport.

3.4. Anti-coagulant properties of flat MMMs with GAGs

The biological anticoagulant activity of the coated MMMs was investigated using PT and aPPT assays, which quantify the speed of blood clotting via the extrinsic coagulation pathway and intrinsic/common coagulation pathways, respectively. When comparing their coagulation time between non-incubated PPP and samples after 1 h incubation with modified MMMs (Fig. S2), all modified MMMs exhibited normal PT (11–15 s) and aPTT (25–35 s) values of coagulation time, with no significant difference between the different GAGs used.

Anti-factor Xa activity was used to investigate the potential anticoagulant activity on the surface of the MMMs. The anti-factor Xa (anti-Xa) assay was adapted to evaluate the potential anticoagulant activity of the MMM after coating or blending with the different GAGs. Results were normalized to the negative control of the assay (initial Xa added), which has no anti-factor Xa properties. Fig. 3-A shows that anti-factor Xa activity of the danaparoid-coated MMMs was significantly increased (~4-fold) compared to the other MMM configurations, which corresponds to improved anti-coagulant properties.

Thrombin is the final and unique protease in the blood coagulation cascade that cleaves the soluble fibrinogen into polymeric fibrin, leading to the clot formation. Therefore, it is important to investigate the thrombi binding and fibrinogen deposition on the different MMMs. Since the DA coated MMM had the best performance in terms of blood coagulation, we also evaluated whether the DA-blended MMM would provide similarly good biocompatibility combined to low danaparoid release. There, the coagulation times obtained from PPP after incubations on the blended MMMs for 1 h were within the physiological ranges, and no different from all the other MMM configurations (Fig. S2). In this case the anti-factor Xa activity of the DA-blended MMMs was significantly superior to the unmodified membranes, but also higher than the heparin-blended membrane used as control (Fig. 3-A). Thrombin binding was similar in the two blended MMMs, but superior to the unmodified membranes (Fig. 3-B). Out of the 6 different MMMs modifications in this study, the DA blended- MMM was the only one with lower fibrinogen deposition (Fig. 3-C), suggesting that this membrane is also superior in reducing final clot formation.

3.5. Flat MMM - activate immune responses and adhesion of blood components

One of the most well-known side effects of HD treatment is the activation of the complement system, thereby leading to C3a and C5a formation that promote recruitment of leukocytes [47]. As shown in Fig. 4A we evaluated the effect complement activation of the various MMMs, by assessing the amount of C5a in serum samples using a commercial sandwich ELISA. After 1 h incubation on the MMMs at 37 °C, serum samples presented similar concentrations of C5a in all modified

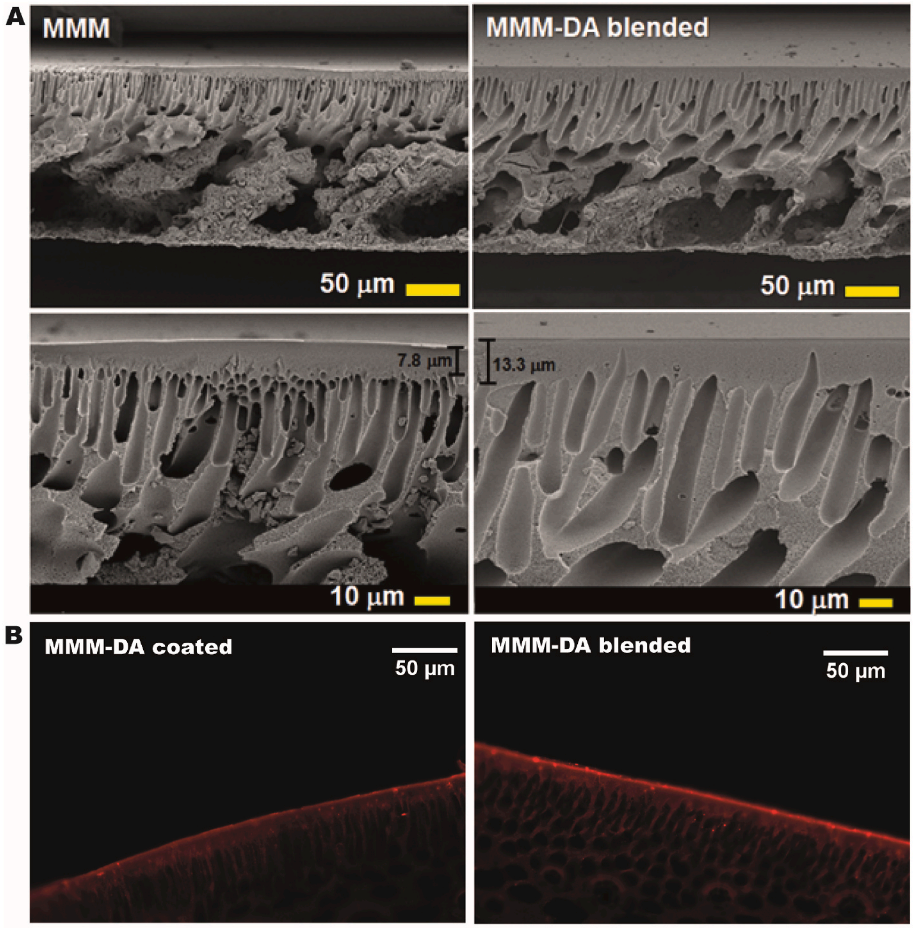

Fig. 2. SEM images of non-blended or blended danaparoid (DA)-MMM with the magnification of x 300 and x 1000 (A). Specific GAG-immunostaining images on MMMs after coating and/or blending danaparoid (B). MMM modifications show fine morphology and homogeneous distribution of GAGs on the membrane surface.

Table 3
Transport characteristics of the unmodified and GAG-modified MMMs. Data are represented as the mean ± standard deviation of at least 2 different samples.

	GAG Source	Water permeance (L/h m^2 bar)	K_{UF} (mL/h m^2 mmHg)	SC_A
	No GAGs	184 ± 68	245 ± 90	0.03 ± 0.03
Coated MMM	HSBK	349 ± 22**	464 ± 30	0.03 ± 0.02
	d-HSBK	184 ± 25	245 ± 33	0.04 ± 0.01
	HS-Glx	177 ± 46	236 ± 62	0.02 ± 0.01
	Danaparoid	228 ± 83	303 ± 110	0.05 ± 0.02
Blended MMM	Danaparoid	165 ± 22	219 ± 29	0.02 ± 0.02
	Heparin	167 ± 13	223 ± 18	0.01 ± 0.01

** indicates statistical significance compared to the unmodified MMM (no GAGs), One-way ANOVA, Dunnet post-hoc. *$p < 0.05$.

MMMs when compared with unmodified membranes. At the same time, these same values were higher than the concentrations of C5a present in serum that was not incubated on any MMM configuration (Fig. 4A). RC cellulose membrane with propensity to activate the complement system [43] was used as positive control. All MMMs had lower level of complement activation compared to serum incubated with the positive control RC membrane (Fig. 4A).

Proteins from the respiratory chain and white blood cells, especially neutrophils, are the most important sources of ROS, and therefore oxidative stress generators. When neutrophils are subjected to the action of foreign agents, they shift to an activated state, significantly increasing the oxygen consumption, thereby producing ROS [48]. Patients on HD display overproduction of ROS [49], which is generated by activated white blood cells, particularly neutrophils [48]. Thus, tight regulation of cell activation is an important aspect for the biocompatibility of HD treatment. Here as shown in Fig. 4B we measured ROS in whole blood samples incubated with the various MMMs for 1 h at 37 °C under shaking, with PMA as positive control. Formation of intracellular ROS was evaluated via chemiluminescence with luminol [50] and data was normalized against the integral luminescence of non-modified MMM (No GAGs, Fig. 4B). The absence of oxidative response by all the MMM goes hand in hand with the lack of neutrophil activation (or any of the other studied blood cell populations).

We also investigated here the potential activation of white blood cells in whole blood after incubation with the different MMM. Cell activation can trigger the expression of adhesion markers by blood cells and platelets and therefore, their adhesion to the dialysis membrane. The accumulation of blood components such as proteins on the membrane surface is an important aspect to consider when assessing the antifouling properties of a synthetic surface [51]. A low platelet adhesion is also crucial for dialysis membranes to maintain the desirable transport and filtration properties [52]. Moreover, platelets play a crucial role in thrombus formation and coagulation [53].

Activation markers CD54 (specific for monocytes, and neutrophils) and CD69 (specific for NK, T and B-lymphocytes) were used to identify

Table 4
Summary of water permeance, protein sieving coefficient, and protein loss and leakage, toxin removal (Cr, IS, and HA for 4 h and 24 h) of HF MMMs ($n_{plasma\ donors} = 3$, $n_{exp.} = 3$). Ultrafiltration coefficients (ml/(m^2 h mmHg)) and protein loss after 24 h HD (g of protein/g of membrane) were placed in brackets. Total protein loss is the amount of protein lost in blood plasma side. The total protein leakage is the amount of protein diffused into the dialysate side, the adsorbed protein is the difference of the total protein loss, and the protein leakage (adsorbed protein = total protein lose-protein leakage).

			FX1000	HF-DA30W
Water permeance (L/(m^2 h bar))	Initial (K_{UF})		96 ± 7 (128)	234 ± 28 (311)
K_{UF}, ml/(m^2 h mmHg)	After 24 h HD (K_{UF})		46 ± 0.1 (61)	97 ± 11 (129)
J/J_0			0.48	0.42
Sieving coefficient, SC	α-lactalbumin		0.85 ± 0.02	0.74 ± 0.11
	β-lactalbumin		0.07 ± 0.08	0.11 ± 0.04
	BSA		0.05 ± 0.01	0.03 ± 0.03
Protein loss and leakage ($g_{protein}/g_{memb}$)	Protein loss, 4 h (24 h)		14.5 ± 2.8 (31.6 ± 10.1)	1.2 ± 0.5 (1.6 ± 1)
	Protein leakage, 4 h (24 h)		11.3 ± 5 (21.9 ± 8.4)	0.12 ± 0.04 (0.7 ± 0.4)
	Adsorbed protein, 4 h (24 h)		3.3 (9.7)	1.04 (0.9)
Toxin removal (mg/m^2 of membrane)	Cr	Total removal, 4 h (24 h)	3533 ± 1526 (6108 ± 2212)	3219 ± 575 (5456 ± 1125)
		Diffusion, 4 h (24 h)	3699 ± 1468 (6280 ± 3110)	920 ± 533 (3051 ± 2320)
		Adsorption, 4 h (24 h)	174 (167)	2299 (2405)
	IS	Total removal, 4 h (24 h)	268 ± 103 (392 ± 97)	412 ± 180 (774 ± 193)
		Diffusion, 4 h (24 h)	174 ± 62 (255 ± 130)	6 ± 2 (48 ± 27)
		Adsorption, 4 h (24 h)	113 (156)	406 (726)
	HA	Total removal, 4 h (24 h)	1747 ± 484 (3456 ± 1399)	1749 ± 384 (2734 ± 823)
		Diffusion, 4 h (24 h)	1577 ± 541 (3180 ± 1115)	394 ± 144 (1938 ± 977)
		Adsorption, 4 h (24 h)	274 (276)	1359 (801)

activated cells by flow cytometry. In addition, blood samples were also incubated with PMA (8 μM) as positive control for activation of T-cells (Fig. 5A), B-cells (Fig. 5B), and NK (Fig. 5C). LPS (10 ng/mL) was used as positive control for activation of neutrophils (Fig. 5D) and monocytes (Fig. 5E). No specific cell activation differences were observed between the different MMMs for any of the white blood cell types. However, both PMA and LPS treatments showed a significant increase of MFI fold change for CD69$^+$ and CD54$^+$ markers respectively, confirming that activation was induced by the positive controls. Notably, there was no activation of immune cells after contact with any of the MMMs, as all the percentages of cell-differentiation/activation double-positive cells were very low (0–8 %) when comparing with their respective positive controls (26–95 %, Table S2).

Finally, we assessed the adhesion of white blood cells (Fig. 6A) and platelets (Fig. 6B) to the different MMMs and observed no significant differences in the adhesion of white blood cells to between the various MMM. However, heparin and DA-blended MMMs significantly decreased platelet adhesion.

The methodology used to count the white blood cells included a sample not incubated with the MMMs, as negative control, to assess the initial number of cells that were added on the membranes at the beginning of the incubation (Fig. 6). Whether or not cells adhered to the polypropylene tube, the adhesion/activation of cells upon contact with the tube would be consistent across all conditions (i.e. baseline). This negative control also allowed us to evaluate whether there was activation of cells due to the staining process. In addition, the method used to stain the different cell markers and proceed with the flow cytometry analysis is a very standardized method that does not include long incubations of the blood in the polypropylene tubes. The staining was performed using an Fc-Block solution to reduce non-specific antibody staining. At the same time, cells incubated with 8 μM of PMA or 10 ng/L of LPS were used as positive control for activation of lymphocytes/monocytes and neutrophils/natural killers, respectively (Fig. 5). A clear activation was shown when using these positive controls, which confirmed that incubation of whole blood on MMMs did not promote white blood cell activation on its own. Since the cell adhesion/activation markers did not increase in the white blood cells, this further confirmed that there was no cell adhesion on the MMM nor to the polypropylene tube.

3.6. HF MMM with DA

3.6.1. HF MMMs morphology

Fig. 7 presents the morphology of the DA incorporated HF MMMs. For all membranes, the sorbents were well distributed within the polymer matrix and the adhesion between the two layers is very good. For the HF-DA60W membranes, some of the micro voids reached the selective inner layer leading to defects. In case of HF-DA30W however, no such defects were observed, hence, we selected these membranes for

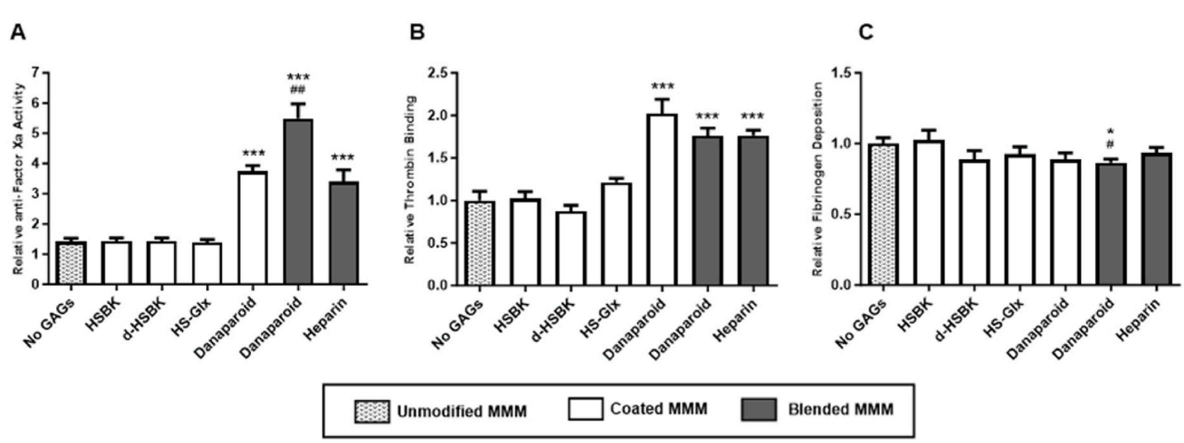

Fig. 3. GAGs modified MMM display superior anti-coagulant properties. A) anti-factor Xa activity was measured after addition of AT and factor Xa to the MMM in PPP plasma. Results were normalized to the negative control. B) Relative thrombin binding and C) fibrinogen deposition were measured after incubation of PPP on the MMM using fluorescently labelled specific antibodies. Results were $^{\#}p < 0.05$; $^{\#\#}p < 0.01$ normalized to unmodified MMM. Results are shown as mean ± standard error of the mean (SEM, n = 3) and compared to unmodified MMM (No GAGs). One-way ANOVA, Dunnet post-hoc. $^{*}p < 0.05$; $^{***}p < 0.001$.

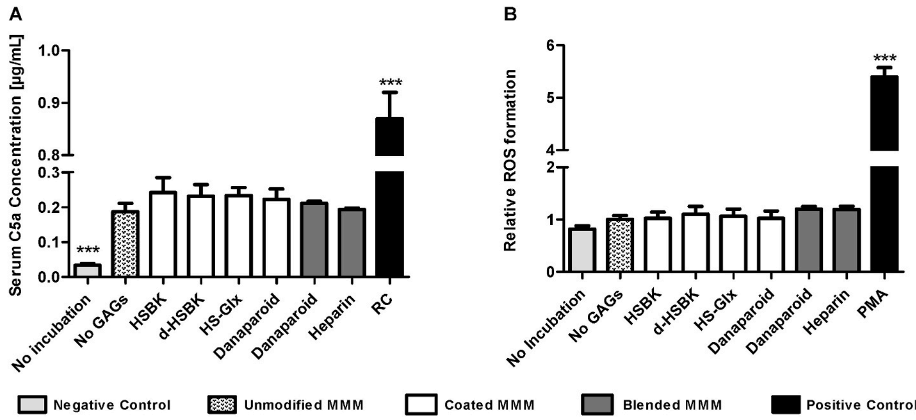

Fig. 4. All MMMs lead to complement activation but not to ROS formation. Activation by the MMM was assessed after 1 h incubation at 37°C. Complement activation was studied by the analysis of C5a concentration in serum samples, whereas serum not incubated with any MMM was included as negative control. Serum samples incubated with regenerated cellulose (RC) membranes under the same conditions were used as positive control (A). Relative formation of ROS was studied in whole blood, normalized the results of unmodified membranes. Whole blood not incubated with any MMM was included as negative control. Whole blood incubated with PMA (8 µM) under the same conditions was used as positive control (B). Results are shown as mean ± standard error of the mean (SEM, n = 3) and compared with unmodified MMM (No GAGs). One-way ANOVA, Dunnet post-hoc. ***p < 0.001.

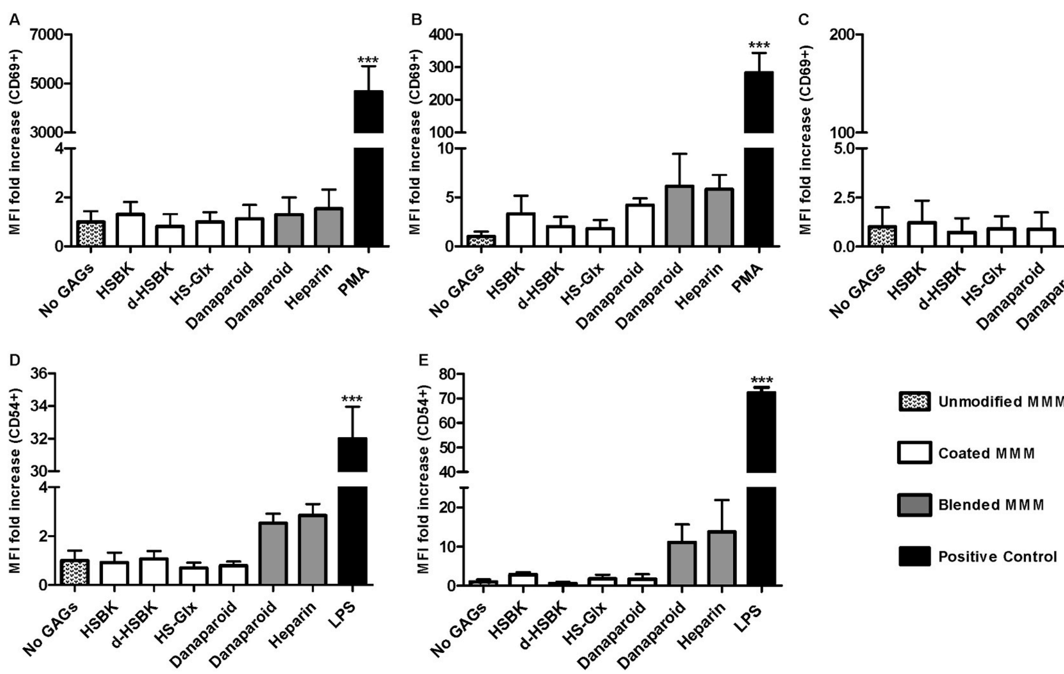

Fig. 5. MMM do not activate immune cells. Activation of T-cells (A), B-cells (B), NK (C), neutrophils (D), or monocytes (C) was assessed by flow cytometry in whole blood for the different MMM configurations, 8 µM PMA (positive control for activation of T-cells, B-cells, and NK) or 10 ng/mL LPS (positive control for activation of neutrophils and monocytes), after 1 h incubation. Cells were analyzed with directly conjugated fluorescent cell differentiation specific antibodies (CD3, CD20, CD56, CD69b, and CD64) and antibodies for specific activation markers (CD69 and CD54). Cell populations were gated using the cell differentiation specific markers. The Median Fluorescence Intensity (MFI) values were multiplied by the percentage of cell-differentiation/cell-activation double-positive cells in the living cell population. Results were normalized to unmodified MMM (No GAGs) for each donor (fold change). Results are shown as mean ± standard error of the mean (SEM, n = 3) and compared to unmodified MMM (No GAGs). One-way ANOVA, Dunnet post-hoc. *p < 0.05; ***p < 0.001.

further characterization (water transport and uremic toxins removal). As shown in Fig. S3, DA for the HF MMMs was mainly located in the inner sorbent free layer. The inner surface was the brightest, but the entire sorbent free layer was stained evenly, which denotes the DA was distributed homogeneously. This staining was not observed in the control HF MMM without GAGs.

3.6.2. HF MMM transport studies

The water permeance of HF-DA30W was much higher compared to the commercial high flux dialyzer (FX1000) (Table 4) whereas the albumin leakage to these membranes was quite comparable. We also investigated the total protein leakage and their fouling potential by comparing their water permeance prior to and after 24 h HD experiments (see Table 4). The water permeance decline after 24 h HD (J/J_0) was quite similar for both membranes, 0.48 for FX1000 and 0.42 for HF-DA30W. Nevertheless, the HF-DA30W had on average higher water permeance (97 L/(m^2 h bar)) after 24 h HD, which is comparable to the initial water permeance of FX1000. Importantly, the HF-DA30W exhibited significantly lower total protein loss from human plasma during 4 h HD compared to FX1000 (1.2 ± 0.5 g/g, vs 14.5 ± 2.8 g/g,

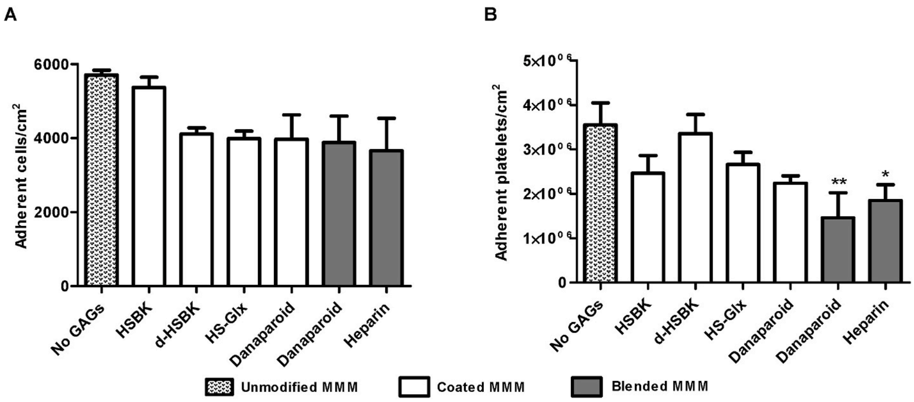

Fig. 6. DA blended MMM is superior in reducing platelet adhesion. The different MMM configurations were evaluated for white blood cell adhesion (A), or platelet adhesion(B). Adhesion of white blood cells/cm^2 (cell consumption) was measured by flow cytometry in whole blood before and after incubation on the MMM for 1 h. Platelet adhesion was measured by LDH quantification. Results are shown as mean ± Standard Error of the mean (SEM, n = 3) and compared with samples incubated with unmodified MMM. One-way ANOVA, Dunnet post-hoc. *$p < 0.05$. **$p < 0.01$.

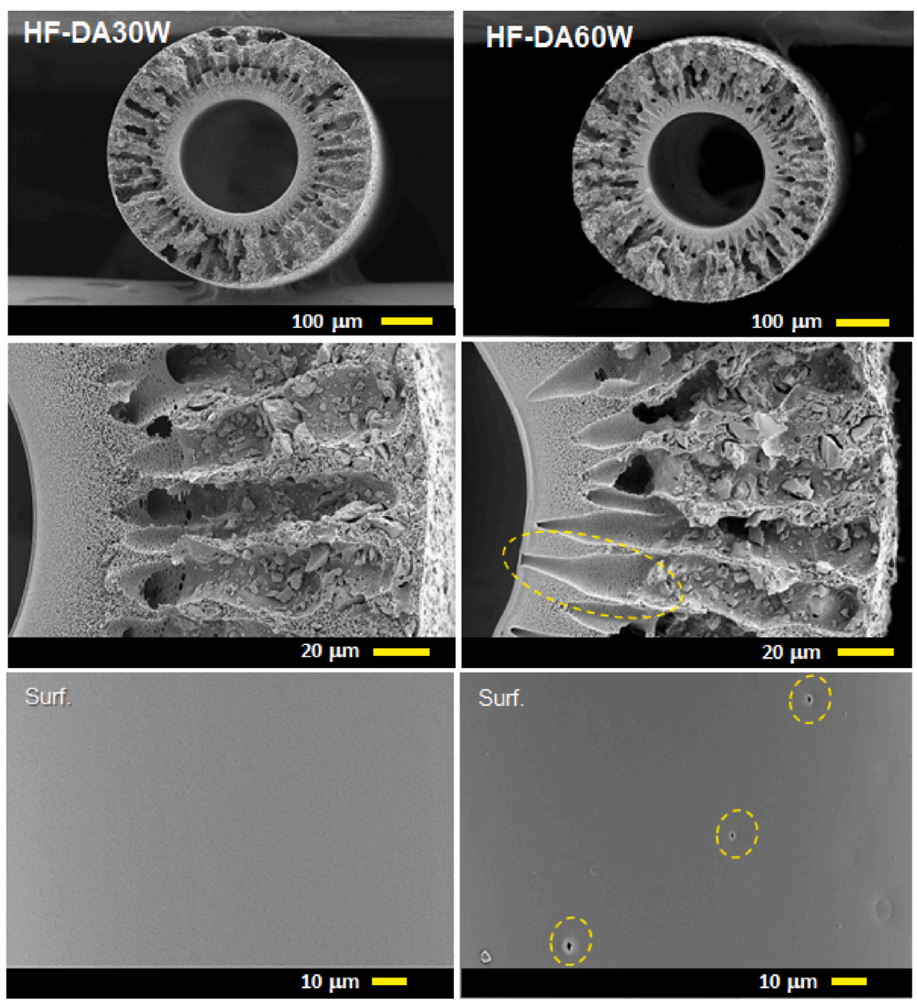

Fig. 7. Membrane morphologies of HF-DA30W and HF-DA60W. The images of the first two row are the cross-sectional images (magnification of x150 and x800), and the third row shows the morphologies of membrane surface (magnification of x1000). The yellow dashed circles indicate the defects of HF-DA60W. (For interpretation of the references to colour in this figure legend, the reader is referred to the Web version of this article.)

see Table 4). This low protein loss of HF-DA30W was mainly due to adsorption (1.04 g/g). In contrast, for the FX1000 it was mainly due to high protein leakage to the dialysate (11.3 ± 5 g/g). These results also support our hypothesis that the incorporation of DA in the membrane selective layer would lead to lower protein adhesion and better hemocompatibility and are consistent to the hemocompatibility studies presented earlier for the flat membranes. Besides, HF-DA30W possess a low albumin leakage (see the results of the protein rejection in Table 4). The combination of the better hemocompatibility and optimal membrane pore morphology may lead to the low protein leakage.

Fig. 8 presents the results of toxin removal by the HF DA30W and FX1000 membranes during 4 h HD. Table 4 summarizes the toxin removal values after 4 h and 24 h of *in vitro* HD. After 4 h HD, the total Cr removal by FX1000 and HF-DA30W were quite similar (3533 ± 1526 and 3219 ± 575 mg/m^2, respectively, $n_{plasma\ donors} = 3$, $n_{exp.} = 3$). However, the main removal mechanism was different; mainly diffusion for FX1000 and mainly adsorption for HF-DA30W. The Cr removal by HF-DA30W was mainly due to adsorption until approximately 2.5 h and the diffusion removal mechanism gradually started afterwards. IS is highly bound to albumin (>93 %), hence it is poorly removed by current dialyzers. In contrast, the MMMs are quite successful in removing IS due to combination of filtration and adsorption [36]. Our results here also support this. The IS removal by FX1000 and HF-DA30W during 4 h HD were 268 ± 103 and 412 ± 180 mg/m^2, respectively (see Fig. 8). Finally, HA binds to protein approximately 40%. The free fraction of HA can easily diffuse from blood to dialysate due to its smaller molecular size comparing to the protein bound HA. This also was observed in this study (see Fig. 8 and Table 4). The HA removal by both membranes during the HD session for 4 h, was comparable, 1747 ± 484 (FX1000) and 1749 ± 384 mg/m^2 (HF-DA30W). The main removal mechanism of HF-DA30W was adsorption and of FX1000 was diffusion.

The errors concerning uremic toxin transport studies, Fig. 8, are larger because they involve use of human plasma from various donors. Especially for the protein bound uremic toxins, their free fraction in plasma can vary per donor leading to variation in concentration gradient across the membrane and hence to variation in removal. Using plasma from various donors is required for properly assessing the performance of the developed membranes compared to commercial ones. These findings are consistent to earlier studies of our group, too [54,55]. Direct comparison of toxin removal to other literature studies is rather difficult due to differences in the applied experimental parameters (*e.g.* the use of blood vs. plasma, the flow rates of blood/plasma and dialysis fluid, the effective membrane surface area, the initial toxin concentrations). However, we believe that these first results are quite promising. Our future research will focus on tailoring the amount of DA to the inner selective layer and testing their performance for solute removal from full blood.

4. Conclusion

In this work we developed new MMMs containing various GAGs aiming to provide membranes with improved blood compatibility combined to high toxin removal.

We firstly prepared flat sheet membranes and found out that DA-modified MMM (coated and blended) showed the best performance concerning blood compatibility and was comparable to heparin blended MMM in terms of coagulation, and platelet adhesion. Importantly, DA-blended membranes had very good stability; showing no significant

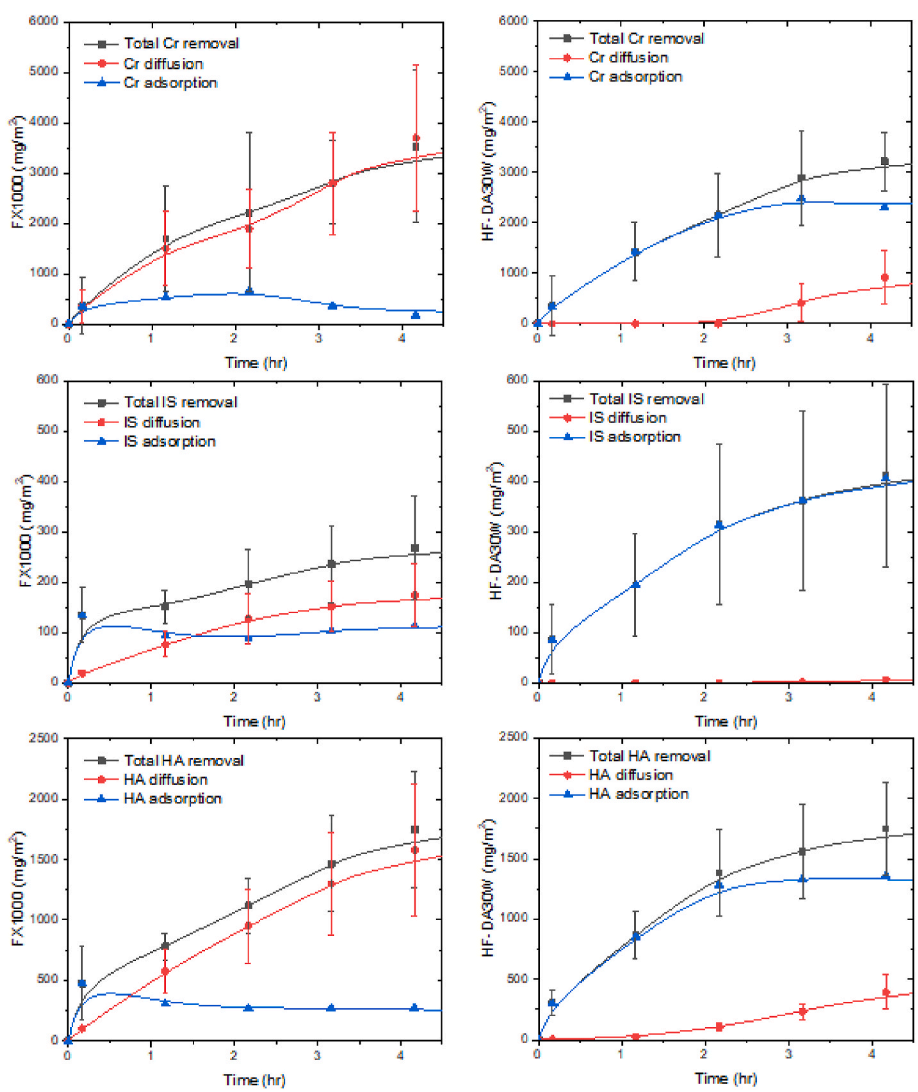

Fig. 8. Removal of toxins such as creatinine, indoxyl sulphate, and hippuric acid during the HD test for 4 h for human plasma ($n_{plasma\ donors} = 3$, $n_{exp.} = 3$).

release of danaparoid.

Based on these findings, we also successfully produced first hollow fiber membranes containing DA. These HF-DA30W exhibit high water permeability, low protein adsorption, low protein leakage compared to commercial FX1000 membranes. Moreover, HF-DA30W showed very good removal of Cr, IS and HA highlighting its potential for application to hemodialysis therapy.

This work has shown the proof of concept of applying DP for developing membranes for good blood compatibility. Since DP is quite expensive, we plan to investigate membrane fabrication protocols that require lower amounts of DP and proceed to performing solute removal tests using full blood.

We think that these membranes could be firstly applicable for patients in IC, for example with acute kidney injury, where rather higher membrane costs could be justified when lowering the risk of bleeding induced by systemic anticoagulation.

CRediT authorship contribution statement

DooLi Kim: Writing – review & editing, Writing – original draft, Methodology, Investigation, Formal analysis, Data curation, Conceptualization. **Maria Margalef:** Writing – review & editing, Writing – original draft, Methodology, Investigation, Formal analysis, Data curation, Conceptualization. **Marissa Maciej-Hulme:** Writing – original draft, Supervision, Methodology, Investigation, Data curation. **Edwin Kellenbach:** Writing – review & editing, Writing – original draft, Methodology, Investigation, Formal analysis, Conceptualization. **Mark de Graaf:** Writing – original draft, Methodology, Investigation, Data curation. **Dimitrios Stamatialis:** Writing – review & editing, Writing – original draft, Supervision, Funding acquisition, Formal analysis, Data curation, Conceptualization, Investigation, Methodology, Project administration. **Johan van der Vlag:** Writing – review & editing, Writing – original draft, Supervision, Project administration, Methodology, Investigation, Formal analysis, Data curation, Conceptualization.

Declaration of competing interest

The authors declare the following financial interests/personal relationships which may be considered as potential competing interests: D. Kim reports financial support was provided by Health Holland. M. Margalef reports financial support was provided by Health Holland. E. Kellenbach reports a relationship with BioChemOss B.V that includes: employment. If there are other authors, they declare that they have no known competing financial interests or personal relationships that could have appeared to influence the work reported in this paper.

Data availability

Data will be made available on request.

Acknowledgements

This work has been supported by the Stichting Life Sciences Health – TKI (Grant no. LSHM16059-SGF (NOVAMEM) and grant LSHM16058-SGF (GLYCOTREAT) both collaboration projects financed by the PPP allowance made available by Top Sector Life Sciences & Health to the Dutch Kidney Foundation to stimulate public-private partnerships).

The authors would like to thank T. H. van Kuppevelt from the Department of Biochemistry in Radboud university medical center for providing HS single chain antibodies (EW4G2 and HS4C3) used in the study.

Appendix A. Supplementary data

Supplementary data to this article can be found online at https://doi.org/10.1016/j.memsci.2024.122669.

References

[1] T. Liyanage, T. Ninomiya, V. Jha, B. Neal, H.M. Patrice, I. Okpechi, M.H. Zhao, J. Lv, A.X. Garg, J. Knight, A. Rodgers, M. Gallagher, S. Kotwal, A. Cass, V. Perkovic, Worldwide access to treatment for end-stage kidney disease: a systematic review, Lancet 385 (9981) (2015) 1975–1982, https://doi.org/10.1016/S0140-6736(14)61601-9.

[2] H. Tam-Tham, R.R. Quinn, R.G. Weaver, J. Zhang, P. Ravani, P. Liu, C. Thomas, K. King-Shier, K. Fruetel, M.T. James, B.J. Manns, M. Tonelli, F.E.M. Murtagh, B. R. Hemmelgarn, Survival among older adults with kidney failure is better in the first three years with chronic dialysis treatment than not, Kidney Int. (2018), https://doi.org/10.1016/j.kint.2018.03.007.

[3] M.K. van Gelder, S.M. Mihaila, J. Jansen, M. Wester, M.C. Verhaar, J.A. Joles, D. Stamatialis, R. Masereeuw, K.G.F. Gerritsen, From portable dialysis to a bioengineered kidney, Expet Rev. Med. Dev. 15 (5) (2018) 323–336, https://doi.org/10.1080/17434440.2018.1462697.

[4] K.N. Ekdahl, I. Soveri, J. Hilborn, B. Fellström, B. Nilsson, Cardiovascular disease in haemodialysis: role of the intravascular innate immune system, Nat. Rev. Nephrol. 13 (2017) 285, https://doi.org/10.1038/nrneph.2017.17.

[5] M. Irfan, A. Idris, Overview of PES biocompatible/hemodialysis membranes: PES-blood interactions and modification techniques, Mater Sci Eng C Mater Biol Appl 56 (2015) 574–592, https://doi.org/10.1016/j.msec.2015.06.035.

[6] Y. Koga, H. Fujieda, H. Meguro, Y. Ueno, T. Aoki, K. Miwa, M. Kainoh, Biocompatibility of polysulfone hemodialysis membranes and its mechanisms: involvement of fibrinogen and its integrin receptors in activation of platelets and neutrophils, Artif. Organs 42 (9) (2018) E246–E258, https://doi.org/10.1111/aor.13268.

[7] M. Kohlova, C.G. Amorim, A. Araujo, A. Santos-Silva, P. Solich, M. Montenegro, The biocompatibility and bioactivity of hemodialysis membranes: their impact in end-stage renal disease, J. Artif. Organs 22 (1) (2019) 14–28, https://doi.org/10.1007/s10047-018-1059-9.

[8] H.F. Ji, L. Xiong, Z.Q. Shi, M. He, W.F. Zhao, C.S. Zhao, Engineering of hemocompatible and antifouling polyethersulfone membranes by blending with heparin-mimicking microgels, Biomater. Sci. 5 (6) (2017) 1112–1121, https://doi.org/10.1039/c7bm00196g.

[9] J.Y. Park, M.H. Acar, A. Akthakul, W. Kuhlman, A.M. Mayes, Polysulfone-graft-poly(ethylene glycol) graft copolymers for surface modification of polysulfone membranes, Biomaterials 27 (6) (2006) 856–865, https://doi.org/10.1016/j.biomaterials.2005.07.010.

[10] M.N.Z. Abidin, P.S. Goh, A.F. Ismail, M.H.D. Othman, H. Hasbullah, N. Said, S. Kadir, F. Kamal, M.S. Abdullah, B.C. Ng, Development of biocompatible and safe polyethersulfone hemodialysis membrane incorporated with functionalized multi-walled carbon nanotubes, Mater Sci Eng C Mater Biol Appl 77 (2017) 572–582, https://doi.org/10.1016/j.msec.2017.03.273.

[11] L.L. Li, C. Cheng, T. Xiang, M. Tang, W.F. Zhao, S.D. Sun, C.S. Zhao, Modification of polyethersulfone hemodialysis membrane by blending citric acid grafted polyurethane and its anticoagulant activity, J. Membr. Sci. 405 (2012) 261–274, https://doi.org/10.1016/j.memsci.2012.03.015.

[12] X. Fu, J.P. Ning, Synthesis and biocompatibility of an argatroban-modified polysulfone membrane that directly inhibits thrombosis, J. Mater. Sci. Mater. Med. 29 (5) (2018), https://doi.org/10.1007/s10856-018-6054-4.

[13] W.C. Lin, T.Y. Liu, M.C. Yang, Hemocompatibility of polyacrylonitrile dialysis membrane immobilized with chitosan and heparin conjugate, Biomaterials 25 (10) (2004) 1947–1957.

[14] C. Wang, R. Wang, Y. Xu, M. Zhang, F. Yang, S.D. Sun, C.S. Zhao, A facile way to prepare anti-fouling and blood-compatible polyethersulfone membrane via blending with heparin-mimicking polyurethanes, Mat Sci Eng C-Mater 78 (2017) 1035–1045, https://doi.org/10.1016/j.msec.2017.04.123.

[15] S.J. Phillips, J.A. Stenken, In situ inner lumen attachment of heparin to poly(ether sulfone) hollow fiber membranes used for microdialysis sampling, Anal. Chem. 90 (8) (2018) 4955–4960, https://doi.org/10.1021/acs.analchem.7b03927.

[16] C.X. Nie, L. Ma, Y. Xia, C. He, J. Deng, L.R. Wang, C. Cheng, S.D. Sun, C.S. Zhao, Novel heparin-mimicking polymer brush grafted carbon nanotube/PES composite membranes for safe and efficient blood purification, J. Membr. Sci. 475 (2015) 455–468, https://doi.org/10.1016/j.memsci.2014.11.005.

[17] C. Sperling, M. Houska, E. Brynda, U. Streller, C. Werner, In vitro hemocompatibility of albumin-heparin multilayer coatings on polyethersulfone prepared by the layer-by-layer technique, J. Biomed. Mater. Res. 76a (4) (2006) 681–689, https://doi.org/10.1002/jbm.a.30519.

[18] V. Hoseinpour, A. Ghaee, V. Vatanpour, N. Ghaemi, Surface modification of PES membrane via aminolysis and immobilization of carboxymethylcellulose and sulphated carboxymethylcellulose for hemodialysis, Carbohydr. Polym. 188 (2018) 37–47, https://doi.org/10.1016/j.carbpol.2018.01.106.

[19] S. Lavaud, E. Canivet, A. Wuillai, H. Maheut, C. Randoux, J.M. Bonnet, J. L. Renaux, J. Chanard, Optimal anticoagulation strategy in haemodialysis with heparin-coated polyacrylonitrile membrane, Nephrol. Dial. Transplant. 18 (10) (2003) 2097–2104, https://doi.org/10.1093/ndt/gfg272.

[20] A.L. Gao, F. Liu, L.X. Xue, Preparation and evaluation of heparin-immobilized poly (lactic acid) (PLA) membrane for hemodialysis, J. Membr. Sci. 452 (2014) 390–399, https://doi.org/10.1016/j.memsci.2013.10.016.

[21] S. Yamamoto, M. Koide, M. Matsuo, S. Suzuki, M. Ohtaka, S. Saika, T. Matsuo, Heparin-induced thrombocytopenia in hemodialysis patients, Am. J. Kidney Dis. 28 (1) (1996) 82–85.

[22] J.D. Esko, S.B. Selleck, Order out of chaos: assembly of ligand binding sites in heparan sulfate, Annu. Rev. Biochem. 71 (2002) 435–471, https://doi.org/10.1146/annurev.biochem.71.110601.135458.

[23] U. Lindahl, J. Couchman, K. Kimata, J.D. Esko, Proteoglycans and sulfated glycosaminoglycans, in: rdA. Varki, R.D. Cummings, J.D. Esko, P. Stanley, G. W. Hart, M. Aebi, A.G. Darvill, T. Kinoshita, N.H. Packer, J.H. Prestegard, R. L. Schnaar, P.H. Seeberger (Eds.), Essentials of Glycobiology, Cold Spring Harbor, NY, 2015, pp. 207–221, https://doi.org/10.1101/glycobiology.3e.017.

[24] C.R. Parish, Heparan sulfate and inflammation, Nat. Immunol. 6 (9) (2005) 861–862, https://doi.org/10.1038/ni0905-861.

[25] A.L. Rops, M.A. Loeven, J.J. van Gemst, I. Eversen, X.M. Van Wijk, H.B. Dijkman, T.H. van Kuppevelt, J.H. Berden, T.J. Rabelink, J.D. Esko, J. van der Vlag, Modulation of heparan sulfate in the glomerular endothelial glycocalyx decreases leukocyte influx during experimental glomerulonephritis, Kidney Int. 86 (5) (2014) 932–942, https://doi.org/10.1038/ki.2014.115.

[26] L. Bode, S. Murch, H.H. Freeze, Heparan sulfate plays a central role in a dynamic in vitro model of protein-losing enteropathy, J. Biol. Chem. 281 (12) (2006) 7809–7815, https://doi.org/10.1074/jbc.M510722200.

[27] J.J. van Gemst, M.A. Loeven, M.J. de Graaf, J.H. Berden, T.J. Rabelink, C.H. Smit, J. van der Vlag, RNA contaminates glycosaminoglycans extracted from cells and tissues, PLoS One 11 (11) (2016) e0167336, https://doi.org/10.1371/journal.pone.0167336.

[28] M.C. Meneghetti, A.J. Hughes, T.R. Rudd, H.B. Nader, A.K. Powell, E.A. Yates, M. A. Lima, Heparan sulfate and heparin interactions with proteins, J. R. Soc. Interface 12 (110) (2015) 589, https://doi.org/10.1098/rsif.2015.0589.

[29] M. Jeansson, B. Haraldsson, Morphological and functional evidence for an important role of the endothelial cell glycocalyx in the glomerular barrier, Am. J. Physiol. Ren. Physiol. 290 (1) (2006) F111–F116, https://doi.org/10.1152/ajprenal.00173.2005.

[30] J.P. Rosengren-Holmberg, J. Andersson, J.R. Smith, C. Alexander, M.R. Alexander, G. Tovar, K.N. Ekdahl, I.A. Nicholls, Heparin molecularly imprinted surfaces for the attenuation of complement activation in blood, Biomater. Sci. 3 (8) (2015) 1208–1217, https://doi.org/10.1039/c5bm00047e.

[31] R. Biran, D. Pond, Heparin coatings for improving blood compatibility of medical devices, Adv. Drug Deliv. Rev. 112 (2017) 12–23, https://doi.org/10.1016/j.addr.2016.12.002.

[32] J.M. Leung, L.R. Berry, H.M. Atkinson, R.M. Cornelius, D. Sandejas, N. Rochow, P. R. Selvaganapathy, C. Fusch, A.K. Chan, J.L. Brash, Surface modification of poly (dimethylsiloxane) with a covalent antithrombin–heparin complex for the prevention of thrombosis: use of polydopamine as bonding agent, J. Mater. Chem. B 3 (29) (2015) 6032–6036.

[33] M. Schindewolf, J. Steindl, J. Beyer-Westendorf, S. Schellong, P.M. Dohmen, J. Brachmann, K. Madlener, B. Potzsch, R. Klamroth, J. Hankowitz, N. Banik, S. Eberle, M.M. Muller, S. Kropff, E. Lindhoff-Last, Use of fondaparinux off-label or approved anticoagulants for management of heparin-induced thrombocytopenia, J. Am. Coll. Cardiol. 70 (21) (2017) 2636–2648, https://doi.org/10.1016/j.jacc.2017.09.1099.

[34] M.S. Tijink, M. Wester, J. Sun, A. Saris, L.A. Bolhuis-Versteeg, S. Saiful, J.A. Joles, Z. Borneman, M. Wessling, D.F. Stamatialis, A novel approach for blood purification: mixed-matrix membranes combining diffusion and adsorption in one step, Acta Biomater. 8 (6) (2012) 2279–2287, https://doi.org/10.1016/j.actbio.2012.03.008.

[35] D. Pavlenko, E. van Geffen, M.J. van Steenbergen, G. Glorieux, R. Vanholder, K.G. F. Gerritsen, D. Stamatialis, New low-flux mixed matrix membranes that offer superior removal of protein-bound toxins from human plasma, Sci Rep-Uk 6 (2016), https://doi.org/10.1038/srep34429.

[36] D. Kim, D. Stamatialis, High flux mixed matrix membrane with low albumin leakage for blood plasma detoxification, J. Membr. Sci. 609 (2020) 118187, https://doi.org/10.1016/j.memsci.2020.118187.

[37] I. Geremia, D. Pavlenko, K. Maksymow, M. Ruth, H.D. Lemke, D. Stamatialis, Ex vivo evaluation of the blood compatibility of mixed matrix haemodialysis membranes, Acta Biomater. 111 (2020) 118–128, https://doi.org/10.1016/j.actbio.2020.05.016.

[38] C. Gardini, E. Urso, M. Guerrini, R. van Herpen, P. de Wit, A. Naggi, Characterization of danaparoid complex extractive drug by an orthogonal analytical approach, Molecules 22 (7) (2017), https://doi.org/10.3390/molecules22071116.

[39] H.N. Magnani, A review of 122 published outcomes of danaparoid anticoagulation for intermittent haemodialysis, Thromb. Res. 125 (4) (2010) e171–e176, https://doi.org/10.1016/j.thromres.2009.10.008.

[40] A.L. Rops, J. van der Vlag, C.W. Jacobs, H.B. Dijkman, J.F. Lensen, T.J. Wijnhoven, L.P. van den Heuvel, T.H. van Kuppevelt, J.H. Berden, Isolation and characterization of conditionally immortalized mouse glomerular endothelial cell lines, Kidney Int. 66 (6) (2004) 2193–2201, https://doi.org/10.1111/j.1523-1755.2004.66009.x.

[41] E.M. van de Westerlo, T.F. Smetsers, M.A. Dennissen, R.J. Linhardt, J.H. Veerkamp, G.N. van Muijen, T.H. van Kuppevelt, Human single chain antibodies against heparin: selection, characterization, and effect on coagulation, Blood 99 (7) (2002) 2427–2433, https://doi.org/10.1182/blood.v99.7.2427.

[42] European Uremic Toxin (EUTox), Uremic toxin - data base. https://database.uremic-toxins.org/soluteList.php, 2023.

[43] F. Knudsen, A.H. Nielsen, J.O. Pedersen, C. Jersild, Activation of complement, generation of C5a, leukopenia and hypoxemia: interlinked membrane-dependent events during hemodialysis, Blood Purif. 2 (2) (1984) 98–107.

[44] X. Ren, L. Xu, J. Xu, P. Zhu, L. Zuo, S. Wei, Immobilized heparin and its anti-coagulation effect on polysulfone membrane surface, J. Biomater. Sci. Polym. Ed. 24 (15) (2013) 1707–1720, https://doi.org/10.1080/09205063.2013.792643.

[45] X.-J. Huang, D. Guduru, Z.-K. Xu, J. Vienken, T. Groth, Blood compatibility and permeability of heparin-modified polysulfone as potential membrane for simultaneous hemodialysis and LDL removal, Macromol. Biosci. 11 (1) (2011) 131–140, https://doi.org/10.1002/mabi.201000278.

[46] H. Baumann, A. Kokott, Surface modification of the polymers present in a polysulfone hollow fiber hemodialyser by covalent binding of heparin or endothelial cell surface heparan sulfate: flow characteristics and platelet adhesion, J. Biomater. Sci. Polym. Ed. 11 (3) (2000) 245–272, https://doi.org/10.1163/156856200743689.

[47] F. Poppelaars, B. Faria, M. Gaya da Costa, C.F.M. Franssen, W.J. van Son, S. P. Berger, M.R. Daha, M.A. Seelen, The complement system in dialysis: a forgotten story? Front. Immunol. 9 (2018) 71, https://doi.org/10.3389/fimmu.2018.00071.

[48] C. Libetta, V. Sepe, P. Esposito, F. Galli, A. Dal Canton, Oxidative stress and inflammation: implications in uremia and hemodialysis, Clin. Biochem. 44 (14–15) (2011) 1189–1198, https://doi.org/10.1016/j.clinbiochem.2011.06.988.

[49] M. Morena, S. Delbosc, A.M. Dupuy, B. Canaud, J.P. Cristol, Overproduction of reactive oxygen species in end-stage renal disease patients: a potential component of hemodialysis-associated inflammation, Hemodial. Int. 9 (1) (2005) 37–46, https://doi.org/10.1111/j.1492-7535.2005.01116.x.

[50] F. Caldefie-Chezet, S. Walrand, C. Moinard, A. Tridon, J. Chassagne, M.P. Vasson, Is the neutrophil reactive oxygen species production measured by luminol and lucigenin chemiluminescence intra or extracellular? Comparison with DCFH-DA flow cytometry and cytochrome c reduction, Clin. Chim. Acta 319 (1) (2002) 9–17.

[51] N. Shahkaramipour, T.N. Tran, S. Ramanan, H. Lin, Membranes with surface-enhanced antifouling properties for water purification, Membranes 7 (1) (2017), https://doi.org/10.3390/membranes7010013.

[52] J.M. Grunkemeier, W.B. Tsai, T.A. Horbett, Co-adsorbed fibrinogen and von Willebrand factor augment platelet procoagulant activity and spreading, J Biomat Sci-Polym E 12 (1) (2001) 1–20. 10.1163/156856201744416.

[53] S. Palta, R. Saroa, A. Palta, Overview of the coagulation system, Indian J. Anaesth. 58 (5) (2014) 515–523, https://doi.org/10.4103/0019-5049.144643.

[54] D.K. Kim, D. Stamatialis, High flux mixed matrix membrane with low albumin leakage for blood plasma detoxification, J. Membr. Sci. 609 (2020) 118187.

[55] O.E.M. ter Beek, M.K. van Gelder, C. Lokhorst, D.H.M. Hazenbrink, B.H. Lentferink, K.G.F. Gerritsen, D. Stamatialis, In vitro study of dual layer mixed matrix hollow fiber membranes for outside-in filtration of human blood plasma, Acta Biomater. 123 (2021) 244–253, https://doi.org/10.1016/j.actbio.2020.12.063.